Model calculation of the frequency and temperature dependence of the electron-spin-resonance linewidth of aluminum

R. H. Silsbee
Laboratory of Atomic and Solid State Physics and Materials Science Center, Cornell University, Ithaca, New York 14853

François Beuneu
Section d'Étude des Solides Irradiés, Centre d'Études Nucléaires, F-92260 Fontenay-aux-Roses, France

(Received 12 October 1982)

The linewidth of the electron-spin resonance in aluminum has been studied experimentally in many laboratories over the frequency range 1.3—80 GHz and at temperatures from 4 to 100 K. At low temperatures the width is thought to be due to motionally narrowed g anisotropy, and at high temperatures spin-flip scattering by phonons is assumed to dominate. Models are developed in this paper, based on previous calculations of the g anisotropy by Beuneu, which give a good semiquantitative account of the linewidth variation over the full range of frequency and temperature.

I. INTRODUCTION

The temperature and frequency dependence of the magnetic resonance of the conduction electrons in aluminum have a number of features which have remained unexplained for a number of years.[1–6] One of the most remarkable features of the existing data is the frequency dependence of the low-temperature linewidth. Data are available at a number of frequencies from 1.27 to 79 GHz, a range of frequencies varying by a factor of 60. The linewidth, either the residual linewidth or the minimum linewidth for those experiments in which the width is observed to increase again at the lowest temperatures, is observed to increase linearly with measuring frequency.

A natural but unsatisfactory explanation is that there is g anisotropy over the Fermi surface described by a $g(\vec{k})$, that electrons with different wave vectors resonate at different fields $H=\hbar\omega/g(\vec{k})\beta$, and that the spread in resonant fields is therefore proportional to the spread in g values and to the frequency of the experiment. At 9 GHz the observed spread in field corresponds to a spread in frequencies of the order of 100 MHz. The difficulty with this explanation is that the electrons are being scattered from place to place on the Fermi surface at a rate of the order of 10^{10} sec^{-1}, as estimated from typical resistivity ratios, so that any given electron samples roughly 20 different k values on the Fermi surface during the relaxation time T_2 characterizing the linewidth. As a result, the resonance line should be motionally narrowed and have an observed width (in frequency) which, using conventional wisdom, would be given by

$$\Delta\omega \sim \frac{\langle(\delta g)^2\rangle}{g^2}\omega_s^2\tau\ , \tag{1}$$

with $\langle(\delta g)^2\rangle$ the mean-square deviation of $g(\vec{k})$ from its mean value g, ω_s the spin procession frequency, and τ a time characterizing the scattering from one k state to another on the Fermi surface.[7] The prediction then is of a quadratic, rather than of a linear dependence upon frequency, a prediction confirmed by experiment for copper and silver,[1] but not for aluminum.

No satisfactory explanation of the linear frequency dependence was proposed until Beuneu[6] calculated explicitly the k dependence of the g shift,

$$\begin{aligned}\delta g(\vec{k}) &\equiv g(\vec{k})-\langle g(\vec{k})\rangle \\ &\equiv g(\vec{k})-g\ .\end{aligned} \tag{2}$$

A remarkable feature of the calculation is the existence of very long tails in the distribution of g shifts, $N(\delta g)$, which extend to values of δg as large as plus and minus several hundred.

The existence of these very large g shifts is a natural consequence of the existence of degeneracy points on the Fermi surface[8] where the second and third zones contact one another in the absence of spin-orbit coupling. The opening of spin-orbit gaps at these points gives rise to locally very small effective masses and hence to exceedingly large orbital moments which, in turn, are strongly coupled to the spin, because it has in fact been the spin-orbit cou-

pling which produced the gap. The very long tails in the g shift distribution $N(\delta g)$ should make one wary of any prediction, such as Eq. (1), which involves the second moment of that distribution because the second moment is likely to be overwhelmingly dominated by the extreme tails.

Beuneu, in a paper hereafter referred to as I,[6] has presented a number of sound physical arguments concerning the linear frequency dependence of the linewidth. The discussion here extends those arguments, making fewer *ad hoc* assumptions, and provides a very natural explanation for the linewidth behavior. Section II of the paper, after a brief summary of Beuneu's results, develops predictions of the frequency and temperature dependence of the electron-spin-resonance (ESR) linewidth in aluminum. These results are compared in Sec. III with the experimental observations and points of agreement and disagreement are noted. There are many points which arise in developing these arguments which complicate the issues significantly, and several are discussed briefly in Sec. IV. Our conclusions are summarized in Sec. V.

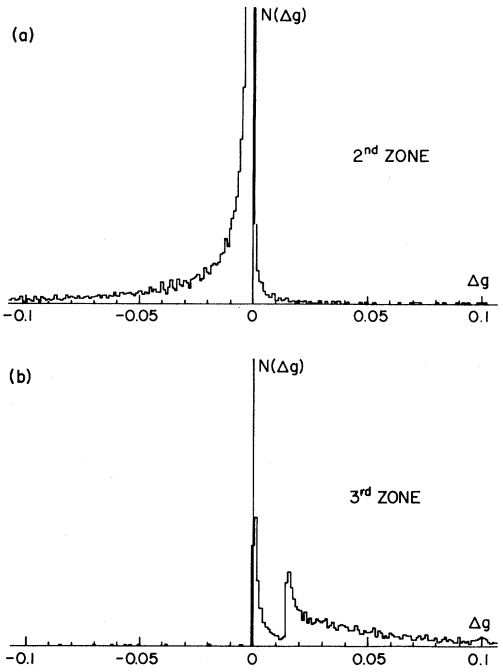

FIG. 1. Distribution of g shifts $N(\delta g)$, as calculated by Beuneu (Ref. 6) for the second and third Brillouin zones in aluminum.

II. A MODEL CALCULATION

A. The g anisotropy

There are a number of important features of Beuneu's results which are reviewed here. Figure 1 gives the histograms individually for the second and third zones of the distribution of g shifts $N(\delta g)$. Note first that the hole surface (2nd zone) has dominantly negative shifts, while the electron surface (3rd zone) has dominantly positive shifts. Thus the assignment of negative (positive) shifts to electrons (holes) that is common in the study of the ESR of defect centers is inconsistent with the calculated shifts in aluminum, as it is occasionally in defect problems.

Second, note that this calculation was performed with the assumption of a positive value of the pseudopotential matrix element V_{111} which enters the Ashcroft theory.[8] It is interesting that a number of papers on aluminum state unequivocally that V_{111} is positive, the ultimate reference for the assertion being the Ashcroft paper in which no comment whatsoever is made concerning the sign, and in which the V_{111} enters all equations quadratically so that the sign is clearly undetermined by any of the arguments in that paper. A reversal of the sign of V_{111} is expected,[6] very roughly, to result in a reflection of the distributions of Fig. 1 about the free-electron g value, giving a second-zone tail extending to positive δg, and a third-zone tail extending to negative g. In this paper, which focuses principally upon the resonance linewidth, the results will not be greatly influenced by changing the sign of V_{111}, and Beuneu's assumption of $V_{111}>0$ will be continued here.

Finally, note that the histograms continue out only as far as g shifts of ± 0.1 but that the ends of the distributions are nowhere in sight. Because of the finite grid spacing in the numerical calculation it is not very helpful to look for the detailed shape of the tails in the extreme wings. The qualitative behavior in the wings, however, is easily estimated. As noted in the Introduction, these tails are a reflection of the degeneracies (R points[8]) on the Fermi surface. Near the R points the g shifts in magnitude are given roughly by

$$\delta g(\vec{k}) \sim \frac{\lambda}{(\lambda^2+e^2k^2)^{1/2}} \frac{\epsilon_F}{(\lambda^2+e^2k^2)^{1/2}} = \frac{\lambda\epsilon_F}{(\lambda^2+e^2k^2)} . \tag{3}$$

λ is the spin-orbit coupling,[6] k here is the distance in k space of $\vec{k}$ from the R point, ϵ_F the Fermi energy, and e the rate of splitting of the two bands as a function of k at the R point in absence of the spin-orbit splitting. $\epsilon_F/(\lambda^2+e^2k^2)^{1/2}$ gives the effective mass enhancement of the orbital magnetic moment for k values near the degeneracy point, and $\lambda/(\lambda^2+e^2k^2)^{1/2}$ gives the strength of mixing of the two bands.[9] Noting that k is the magnitude of a two-dimensional displacement vector, along the Fer-

mi surface in any direction from the R point, the density of k states on the Fermi surface near the R points may be written as

$$N_1(k)dk \sim 2\pi k\, dk/4\pi k_F^2 ,$$

from which it follows that

$$N(\delta g)=\begin{cases} N_1(k)\dfrac{dk}{dg}\approx \dfrac{1}{16}\dfrac{\lambda}{\epsilon_F}\dfrac{1}{(\delta g)^2}, & \delta g<\delta g_m\sim\dfrac{\epsilon_F}{\lambda} \\ 0, \quad \delta g>\delta g_m\ . \end{cases} \tag{4}$$

Detailed numerical coefficients have not been calculated in making these estimates. Noting that there are 24 R points on the Fermi surface, one may estimate the contribution from the tails to the mean-square g shift as

$$\langle(\delta g)^2\rangle \sim \int_0^{\delta g_m}(\delta g)^2\frac{\lambda}{\epsilon_F}\frac{1}{(\delta g)^2}d(\delta g)\sim 1 , \tag{5}$$

recalling $\delta g_m \sim \epsilon_F/\lambda$. Comparison with the value determined in I, $\langle(\delta g)^2\rangle = 0.22$, shows clearly that it is the extreme tails of the g distribution which dominate the moment. The apparent disagreement is of no significance without a more careful calculation of the numerical constants in Eq. (3).

Remarkable is the fact that $\langle(\delta g)^2\rangle$ does not depend upon λ. The result emphasizes both the danger in arguing that $\langle(\delta g)^2\rangle$ is simply related to spin-orbit energies and typical band splittings, and the importance in ESR of possible degeneracies in the polyvalent metals, a point suggested by Beuneu and Monod[10] in a survey of ESR results in metals.

B. A free-electron simulation of the aluminum problem

In the preceding section it was noted that practically all of the second moment of the $g(\vec{k})$ distribution in aluminum is contributed by those portions of the Fermi surface, in both the second and third zones, which are near the zone contact points, or R points. This suggests the use of the following, rather oversimplified but easily calculable, model to illustrate the important physical ideas underlying the conduction spin relaxation in aluminum.

The model is illustrated in Fig. 2. The electrons are taken as a free-electron gas with Fermi sphere radius k_F and cyclotron frequency $\omega_c=(eB)/m^*c$, with B the applied magnetic field. Almost anywhere on the Fermi surface the g shift is taken to be zero, but over a few small selected areas, referred to as the R disks, the g shift is taken to be large and constant, δg_0. The radius κ of the R disks is appropriately taken to give a disk area $\pi\kappa^2$ equal to the

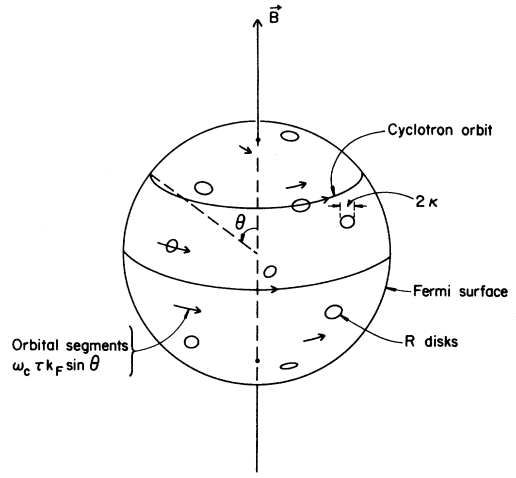

FIG. 2. Schematic view of the free-electron Fermi surface in aluminum with randomly distributed R disks (see text), cyclotron orbits, and orbital segments as limited by the resistivity scattering.

area, near the R points, of the real Fermi surface in aluminum over which the energy gap is dominantly determined by the spin-orbit interaction. δg_0 might be taken to be a suitable average over this region of the real $\delta g(k)$, though in fact it will be determined by a somewhat more complex argument. For the moment, the magnitudes of κ and δg_0 may be thought of as given roughly by

$$\kappa/k_F \sim 10^{-3} , \tag{6a}$$

$$|\delta g_0| \sim 10^{+3} . \tag{6b}$$

The sign of δg_0 is of little import in this discussion, but is most conveniently thought of as positive on one-half of the disks, negative on the rest, to leave a mean g shift of zero.

There are 48 R points on the Fermi surface of aluminum, 24 on each of the second- and third-zone surfaces, after lifting of the R degeneracy by the spin-orbit splitting. In the model the 48 R disks are supposed to be randomly distributed over the sphere, the randomization to simplify the calculation by avoiding the need to keep track of whether or not particular cyclotron orbits traverse only one or several R disks. Because of the small value of κ, the probability of a given cyclotron orbit traversing more than one disk is small and the consequences of a double traversal are neglected. In randomizing the distribution, possible anisotropy in the linewidth is of course omitted from the model.

Individual electrons are assumed to scatter randomly from point to point on the Fermi surface at a rate $1/\tau$, while between scattering events they move in cyclotron orbits on the Fermi surface with a

linear velocity in k space,

$$|\dot{\vec{k}}| = \omega_c k_F \sin\theta \ , \tag{7}$$

with θ the angle between the electron wave vector $\vec{k}$ and the applied field $\vec{B}$.

C. Solutions for this model

The arguments for the magnitude of the motionally narrowed conduction-electron-spin-resonance (CESR) linewidth depend crucially upon the magnitude of the typical orbital segment length in k space, $\omega_c \tau k_F$, traversed by an electron between scattering events. The results discussed below fall naturally into three different regimes, appropriately defined by this parameter.

The high-temperature region is defined by the relation

$$\omega_c \tau k_F \ll \kappa \ , \tag{8}$$

or the requirement that the orbital segments on the Fermi surface be small compared with the radius of an R disk. In this regime the electrons are scattered on and off the disks much more rapidly than they move on and off the disks as a consequence of their cyclotron motion, and hence the effects of the cyclotron motion are negligible. In *this* regime the conventional result for motional narrowing is appropriate. Noting that in the model the rms spread in g values is given by

$$\langle (\delta g)^2 \rangle = (\delta g_0)^2 (48\pi\kappa^2 / 4\pi k_F^2) \ , \tag{9}$$

the conventional narrowing result for the linewidth gives

$$\frac{1}{T_{mz}} = \left\langle \left[\frac{\delta g}{g} \right]^2 \right\rangle \omega_s^2 \tau = 12 \frac{(\delta g_0)^2}{g^2} \frac{\kappa^2}{k_F^2} \omega_s^2 \tau \ . \tag{10}$$

$1/T_{mz}$ denotes the contribution of the motionally averaged g anisotropy to the full linewidth $1/T_2$, assuming, for the present, a scalar g shift rather than tensor.

This result is inappropriate in the intermediate-temperature regime $\kappa \ll \omega_c \tau k_F \ll k_F$ because in this regime the correlation time for the narrowing is determined not by the time between collisions, but by the average time spent on the R disks, which is now determined by the speed of the cyclotron orbital motion, not the collision rate. An approximate result is obtained by the replacement of τ in Eq. (10) by the disk transit time $\tau_{\text{transit}} \approx \kappa / k_F \omega_c$. Note that the resultant expression for the width varies as ω_s^2 / ω_c and is therefore linearly proportional to the field at which the experiment is performed, and a natural explanation is obtained for the experimentally observed linear dependence of linewidth upon frequency. Further, the coefficient of proportionality does not involve τ, in accord with the experimental result that the slope of the plot of linewidth versus frequency is nearly independent of temperature.[5]

A more quantitative result is easily obtained. The precession phase, relative to the mean phase of all of the spins, accumulated by an electron in an orbit of polar angle θ as it traverses a disk along a trajectory with impact parameter δk, is

$$\phi(\theta, \delta k) = \left[\frac{\delta g_0}{g} \omega_s \right] \frac{2(\kappa^2 - \delta k^2)^{1/2}}{\omega_c k_F \sin\theta} \ . \tag{11}$$

The rate at which any given electron meets R disks, if it is in orbit of polar angle θ, is

$$R(\theta) = (\omega_c k_F \sin\theta) \frac{48 \times 2\kappa}{4\pi k_F^2} \ , \tag{12}$$

where $(48/4\pi k_F^2)$ is the R-disk density, 2κ its collision cross section, and $\omega_c k_F \sin\theta$ the electron's k velocity. The rate at which the electrons gain mean-square precession phase error is then given by

$$\frac{d}{dt} \langle \phi^2(t) \rangle \equiv \frac{1}{4\pi} \int_0^{\pi} 2\pi \sin\theta \, d\theta \, R(\theta) \times \langle \phi^2(\theta, \delta k) \rangle_{\delta k} \ , \tag{13}$$

where $\langle \ \rangle_{\delta k}$ is the average of Eq. (11) over impact parameters $-\kappa < \delta k < \kappa$. Equation (13) is easily evaluated if $\sin\theta$ is assumed constant over the disk, which is reasonable for $\kappa \ll k_F$, and with the results of Abragam[11] gives

$$\frac{1}{T_{mz}} = \frac{1}{2} \frac{d}{dt} \langle \phi^2 \rangle = 16 \left[\frac{\delta g_0}{g} \omega_s \right]^2 \frac{\kappa^3}{k_F^3} \frac{1}{\omega_c} \ . \tag{14}$$

Finally, the low-temperature regime is characterized by the condition $\omega_c \tau \gg 1$, for which the electron moves in a single cyclotron orbit for a number of periods before scattering to a new orbit. The cyclotron motion now gives effective averaging over the full orbit of the g variation associated with the R disk for those orbits which traverse a disk. The orbitally averaged g shift for an orbit with polar angle θ which traverses a disk on an orbit with impact parameter δk is

$$\delta g(\theta, \delta k) = \delta g_0 \frac{2[\kappa^2 - (\delta k)^2]^{1/2}}{2\pi k_F \sin\theta} \ . \tag{15}$$

The probability of an orbit of polar angle θ traversing a disk is

$$P(\theta) = \frac{2\kappa 2\pi k_F \sin\theta}{4\pi k_F^2} \times 48 \ , \tag{16}$$

which allows the calculation of the appropriate average over the Fermi surface of the mean-square orbi-

tally averaged g shifts as

$$\langle[\delta g(\theta,\delta k)]^2\rangle_{\rm FS}=\frac{1}{4\pi}\int_0^\pi 2\pi\sin\theta\,d\theta\,P(\theta)\times\langle[\delta g(\theta,\delta k)]^2\rangle_{\delta k}\equiv\langle g_0^2\rangle\ . \tag{17}$$

This gives, finally, for the low-temperature regime

$$\frac{1}{T_{mz}}=\frac{\langle[\delta g(\theta,\delta k)]^2\rangle_{\rm FS}}{g^2}\omega_s^2\tau=\frac{16}{\pi}\left[\frac{\delta g_0}{g}\omega_s\right]^2\frac{\kappa^3}{k_F^3}\tau\ . \tag{18}$$

The considerations up to this point have tacitly assumed a scalar g shift and have thus dealt only with the fluctuations in the z component of the effective field felt by the spins through the g-anisotropy contributions $\delta g_{zz}(\vec{k})$. There will also be transverse components of the effective field felt by the spins arising from off-diagonal elements of the g-shift tensor, $\delta g_{zx}(\vec{k})$ and $\delta g_{zy}(\vec{k})$. These elements of the g tensor contribute to the relaxation of both the longitudinal (z) and transverse (y and x) components of the spins and hence also contribute to the linewidth (see Ref. 12, Sec. 5.7). Qualitative considerations based on the work of I suggest that typical off-diagonal elements of the g-shift tensor are comparable in magnitude to the diagonal elements; this implies,[12] in the limit of short correlation time $\omega_c\tau\ll 1$, an additional contribution to the linewidth comparable in magnitude to $1/T_{mz}$ as well as a contribution to the longitudinal relaxation $1/T_1$. The situation is more complex, depending critically upon ω_s/ω_c, for long correlation times as noted briefly in Sec. IV B. For the present analysis and comparison with the data it is adequate simply to increase all of the rates calculated above by a factor of 2, $1/T_m\approx 2/T_{mz}$, with $1/T_m$ the full predicted width due to motional narrowing of the full g-shift tensor. With this modification, the results in the three regimes are conveniently summarized by introducing the definition

$$A\equiv 2\left[\frac{(\delta g_0)^2}{g^2}48\frac{\pi\kappa^2}{4\pi k_F^2}\right]\frac{\omega_s}{\omega_c}\ , \tag{19}$$

where A, apart from the factor $\omega_s/\omega_c\approx 1$, is the mean-square fractional g shift over the Fermi surface. The linewidths, expressed as a fraction of the resonance field, are then for high temperature

$$\frac{1}{\omega_s T_m}=A(\omega_c\tau)\ , \tag{20a}$$

for intermediate temperature

$$\frac{1}{\omega_s T_m}=\frac{4}{3}A\frac{\kappa}{k_F}\ , \tag{20b}$$

and for low temperatures

$$\frac{1}{\omega_s T_m}=\frac{4}{3\pi}A\frac{\kappa}{k_F}(\omega_c\tau)\ . \tag{20c}$$

The values of $\omega_c\tau$ dividing one regime from the next are

$$(\omega_c\tau)_{H\text{-}I}=\frac{4}{3}\frac{\kappa}{k_F}\ , \tag{21a}$$

$$(\omega_c\tau)_{I\text{-}L}=\pi\ , \tag{21b}$$

where H represents high temperature, I represents intermediate temperature and L represents low temperature. These results are summarized schematically by the straight line segments of Fig. 3, and again we emphasize that the result of Eq. (20b), valid over a range of the order of 10^3 in $\omega_c\tau$, gives naturally the prediction of a fractional linewidth independent of frequency, or equivalently, a linewidth proportional to frequency, over a wide range of scattering times τ.

D. The Freedman-Fredkin formalism

The results of Freedman and Fredkin (FF),[13] with the neglect of exchange, can also be applied to the model to give essentially the same results, but a

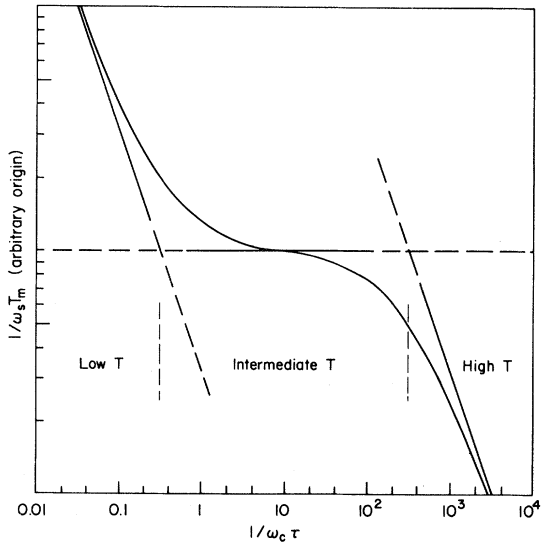

FIG. 3. Schematic representation of the dependence of the motionally narrowed linewidth vs scattering rate for the R-disk model described in the text; the straight-line segments correspond to the several limiting behaviors discussed in Sec. II C; the curve is a simple interpolation scheme.

somewhat different viewpoint of the physics. Crucial in the FF development is the Fourier expansion of the g shift as seen by an electron as it traverses its cyclotron orbit, Eq. (4.4) of FF. For the model discussed here, with constant velocity $\omega_c k_F \sin\theta$ around the cyclotron orbit of polar angle θ, it is convenient to define the Fourier amplitudes by

$$\delta g(k) = \sum_{m=-\infty}^{\infty} g_m \exp(imk/k_F \sin\theta) , \tag{22}$$

where the g_m will depend both upon the polar angle θ of an orbit, and the impact parameter δk of those orbits which intersect the R disks. All g_m are of course zero for orbits which do not traverse the disks. Note that in Eq. (22) the g_0 are the orbitally averaged g shifts discussed briefly [see Eq. (17)] in obtaining the low-temperature result in the preceding section, and are not the full average of g over the Fermi surface which is denoted simply by g without a subscript.

For Fourier components at frequencies whose period is long compared with the transit time through the R disks, the Fourier amplitudes $g_m(\theta,\delta k)$ for given θ and δk are all equal in magnitude and are given directly by Eq. (15), i.e.,

$$|g_m(\theta,\delta k)| = g_0(\theta,\delta k) \tag{23}$$

for small m, and averaging over δk and θ gives

$$\langle |g_m(\theta,\delta k)|^2 \rangle = \frac{16}{\pi}\frac{\kappa^3}{k_F^3}(\delta g_0)^2 \tag{24}$$

for small m.

The Fourier amplitudes fall off for large m, namely when the period of the oscillation,

$$\exp(imk/k_F \sin\theta) ,$$

in k becomes comparable with the disk diameter 2κ. More specifically, the cutoff m, denoted m_c, for orbits with $\delta k = 0$, $\theta = \pi/2$, is

$$m_c = \pi k_F/\kappa . \tag{25}$$

This is an adequate estimate for all orbits for the purpose of the following discussion.

FF equation (4.8), deleting the exchange terms and adapting to the notation of this paper, gives the linewidth in terms of the Fourier amplitudes g_m as

$$\frac{1}{T_{mz}} = \lim_{\omega\to 0}\left[\sum_{m=-\infty}^{\infty}\frac{\langle |g_m|^2\rangle}{g^2}\omega_s^2\frac{\tau}{1+(\omega-m\omega_c)^2\tau^2}\right] \tag{26}$$

$$= \sum_{m=-\infty}^{\infty}\frac{\langle |g_m|^2\rangle}{g^2}\omega_s^2\frac{\tau}{1+(m\omega_c\tau)^2} . \tag{27}$$

The form of Eq. (26) is introduced to emphasize that the result, Eq. (27) of FF, is the zero-frequency component of the spectral density sketched in Fig. 4. Again Eq. (27) is easily evaluated in three regimes of τ.

Starting this time with the low-temperature regime $\omega_c\tau \gg 1$, the many peaks in the spectral density of Fig. 4 are well resolved, and only the $m=0$ term in the sum contributes to the zero-frequency spectral density, which, in this limit, gives

$$\frac{1}{T_{mz}} = \frac{\langle g_0^2\rangle}{g^2}\omega_s^2\tau , \tag{28}$$

which is just the result Eq. (18).

If $\kappa/k_F \ll \omega_c\tau \ll 1$, the peaks in Fig. 4 overlap strongly, but the wings of the peaks for small m do not extend out as far as the cutoff frequencies $m_c\omega_c$. In this regime the spectral density at zero frequency is independent of τ; the sum on m in Eq. (27) may be converted to an integral which is independent of the cutoff m_c for $m_c\omega_c\tau \gg 1$ to give, using Eq. (24),

$$\frac{1}{T_{mz}} = \pi\frac{\langle |g_m|^2\rangle}{g^2}\frac{\omega_s^2}{\omega_c} = 16\left[\frac{\delta g_0}{g}\omega_s\right]^2\frac{\kappa^3}{k_F^3}\frac{1}{\omega_c} , \tag{29}$$

which is the result Eq. (14).

Finally, for $\omega_c\tau \ll 1/m_c = \pi k_F/\kappa$, each peak in Fig. 4 extends far beyond the cutoff frequency $m_c\omega_c$, and the sum of Eq. (27) is again easily evaluated to give

$$\frac{1}{T_{mz}} = \omega_s^2\tau\sum_{m=-\infty}^{\infty}\frac{\langle |g_m|^2\rangle}{g^2} = \left\langle\left[\frac{\delta g}{g}\right]^2\right\rangle\omega_s^2\tau , \tag{30}$$

namely Eq. (10). Before comparing these results with the experimental data it is useful to present some arguments concerning the "phonon-induced spin-flip scattering."

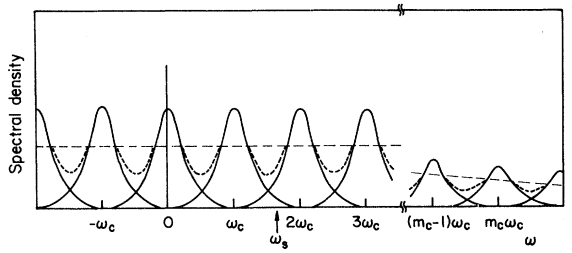

FIG. 4. Spectral density function appearing in Eq. (26). The solid lines indicate the individual components entering the sum of Eq. (26), the short dashed lines are the sum of these overlapping contributions for the case illustrated with $\omega_c\tau \equiv 4$, and the long dashed line is the spectral density when the overlap is large, $\omega_c\tau \ll 1$, but still $\omega_c\tau \gg 1/m_c$.

E. Phonon-induced relaxation

The previous sections are concerned with the motional narrowing of the g anisotropy in aluminum. A second important feature of the experimental results is the increase in linewidth at high temperature, the phonon-induced relaxation. The model suggested above also implies an easily calculable phonon-induced relaxation rate, which will be denoted $1/T_p$. Although it turns out that the R disks do not dominate the process sufficiently that the model is adequate, the R-disk model is conveniently illustrative of the essential physics, and appropriate modifications to it are indicated at the end of the section.

In the regions within a distance κ of the R points, the wave functions for the conduction electrons are roughly equal mixtures of spin-up and spin-down components k, since the R point is a point of a spin-orbit-induced gap. Far from the R points, however, the wave functions are almost purely spin up or purely spin down. Consider a phonon scattering process in which the electron-phonon interaction potential is supposed to contain no spin dependence. Any scattering between the neighborhood of an R point and elsewhere on the Fermi surface, scattering either to or from the R neighborhood, will result in randomization of the spin since the scattering involves the matrix element of a spin-independent potential between a state with an equal mixture of spin up and spin down and a state which is either pure spin up or pure spin down.[14,9] In this crude model of the R disks the resultant phonon-induced relaxation rate is simply

$$\frac{1}{T_p}=(48\pi\kappa^2/4\pi k_F^2)/\tau\ . \tag{31}$$

Unfortunately, the model, though illustrating the important physics, does not give a correct quantitative estimate of the phonon-induced relaxation. As discussed briefly below this is because the strength of the weighting of this process near the R points does not overwhelm the contributions from elsewhere on the Fermi surface, as it does for the motional narrowing contributions to the width.

Consider, instead of the R disks, the ridges at the intersection of the square-like and hexagonal-like sections of the second-zone Fermi surface. Along these ridges the second-zone surface is split from the next higher band by a crystal-field matrix element of the order of V_{111}, but which vanishes (apart from the spin-orbit splitting) because of symmetry at the R points which terminate these ridges. V_{111} is not very large, ~ 0.0179 Ry, compared with the spin-orbit splitting of the bands, $\lambda\sim 0.001$ Ry, at the R points. Thus there is substantial spin-orbit mixing along and in the neighborhood of these ridges, and, as in the discussion of the previous paragraph, spin flips associated with the spin mixing for states on the ridges and scattering into or out of these states from or into states elsewhere on the Fermi surface with nearly pure spin states are thought to dominate the phonon-induced relaxation observed at high temperature.

In more detail, one estimates the relaxation rate associated with scattering onto, and subsequently off of, the (111) ridges on the Fermi surface using the formula

$$\frac{1}{T_p}=\int_{\text{single (111) ridge}}\frac{2\lambda^2}{\epsilon^2(k_\perp,k_{||})}\times\frac{1}{\tau}\frac{dk_\perp dk_{||}}{4\pi k_F^2}\times 48\times 2\ . \tag{32}$$

A two-dimensional integral is taken along a (111) ridge from one R point to a neighboring R point. $k_{||}$ is a coordinate along the ridge, and $k_\perp$ is perpendicular to the ridge. $\epsilon(k_\perp,k_{||})$ is the gap between the nearly degenerate bands which dominate the g shift for k on the ridges, and is obtained from the calculations of I. The effective full width of the ridges, the range of $k_\perp$ over which ϵ^2 is within a factor of 2 of its maximum value on the ridge crest, is of the order of 5% of k_F, becoming narrower as the R point is approached. λ is one-half of the spin-orbit gap at the R point, and is taken from I to be $\lambda=3.8\times 10^{-4}$ Ry. In Eq. (32), λ^2/ϵ^2 is the probability of a spin flip associated with scattering from (to) a pure spin state to (from) a state with spin mixing λ/ϵ. A factor of 2 is included to account for the fact that the spin flip can occur either on scattering to or from the elements $dk_\perp dk_{||}$. $1/\tau$ is the scattering rate, and $dk_\perp dk_{||}/4\pi k_F^2$ is the probability that a scattering be to the element $dk_\perp dk_{||}$. A factor of 48 gives the number (including both second and third zones) of (111) ridges on the Fermi surface. The final factor of 2 is the usual factor of 2 relating relaxation rate $1/T_1$ to spin-flip rates.[12] Evaluation of Eq. (32) using the techniques of I yields

$$\frac{1}{T_p}=\frac{2\times 10^{-4}}{\tau}\ . \tag{33}$$

The greater importance of the ridge relative to the R points in this T_1 process as compared with the motional narrowing process may be argued as follows. From Eq. (32), estimating the integral along $k_\perp$ across the ridge, the contribution to $1/T_p$ from the element $dk_{||}$ along the ridge may be shown proportional to $1/\epsilon(k_{||})$ where $\epsilon(k_{||})$ is the energy gap on the crest of the ridge. Noting that near the R points $\epsilon(k_{||})$ varies linearly with distance from the R point, one sees that the integral over $k_{||}$ diverges

logarithmically, implying significant contributions from all of the ridge. One can also extend the arguments concerning the motionally narrowed g shifts to orbits which cross the (111) ridges. Arguments analogous to those leading to Eq. (11) and (13) give a contribution to $1/T_{mz}$ from a ridge element $dk_{||}$ proportional to $1/\epsilon(k_{||})^2$. This gives a stronger divergence at the R point than for the calculation of $1/T_p$, indicating the dominance of the immediate neighborhood in determining the motionally narrowed width $1/T_m$.

III. APPLICATION TO CESR IN ALUMINUM

A. Scaling

In the preceding section estimates have been made both of the ESR width due to motional narrowing of the g anisotropy [Eqs. (20) and (21),] and of the width due to relaxation associated with phonon (or impurity) scattering, [Eqs. (32) and (33)]. The results (20) and (21) are naturally represented in the scaled form $1/\omega_s T_m = F(\omega_c \tau)$, and Eq. (33) is easily forced into a similar form by writing

$$1/\omega_s T_p = 2\times 10^{-4}(\omega_c/\omega_s)/\omega_c\tau$$

to give for the predicted width $1/T_2$ the sum of the two contributions

$$\frac{1}{\omega_s T_2} = F(\omega_c\tau) + \frac{2\times 10^{-4}(\omega_c/\omega_s)}{\omega_c\tau} . \qquad (34)$$

An important confirmation of these ideas would be the demonstration of this scaling in the existing linewidth data for aluminum. Unfortunately, that is not possible without knowing independently the scattering rate $1/\tau$. Figure 5 represents an attempt to reveal this scaling with a minimum of data manipulation. At high temperatures one knows that phonon scattering dominates over impurity scattering, and further that the phonon scattering rate, at temperatures well below the Debye temperature, is expected[15] to vary as T^3. If the data are plotted versus $\omega_c^{-1}T^3$, then at least in the regime in which $1/\tau$ is dominated by phonon rather than impurity scattering, such a plot should reveal the scaling implied by Eq. (34).

Figure 5 gives a log-log plot of the relative width $1/\omega_s T_2$ vs $\omega_c T^3$ for data taken over the frequency range from 1.27 to 80 GHz,[1–5] and with the horizontal axis also explicitly labeled as temperature for three of the different frequencies. The plotted points are taken from the smoothed curves in figures of published results and are not actual data points. The figure does not include all available data, but is selected to include results at a wide variety of frequencies, namely six, and from four different laboratories.

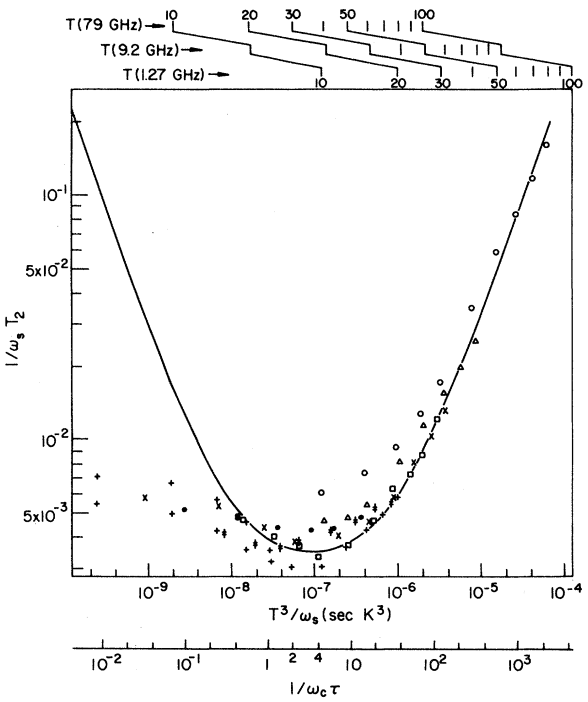

FIG. 5. Scaled linewidth $1/\omega_s T_2$, as a function of T^3/ω_s for the ESR in aluminum. Data are taken at the following frequencies: ○, 1.27 GHz (Ref. 1); △, 9.3 GHz (Ref. 1); ●, 9.3 GHz (Ref. 2); ×, 21.0 GHz (Ref. 3); □, 35.0 GHz (Ref. 1); ∓, 60.0 GHz (Ref. 4); +, 79.0 GHz (Ref. 5). The solid line is the fitted theoretical universal curve. The scales at the top of the graph convert the abscissa to a temperature scale for the data corresponding to three of the experimental frequencies. The scale at the very bottom converts the abscissa to a scattering rate expressed in units of ω_c, under the assumption of a value $p = 2.1\times10^7$ sec^{-1}K^{-3} of the constant in Eq. (35), and a value of 1.6 for ω_s/ω_c.

No attempt has been made to correct the data for the effects of surface relaxation or of residual impurity scattering. The residual scattering is of course the dominant contribution to the resistivity at the lowest temperature at each frequency. The effect of correcting for the residual scattering is to shift the lower-temperature points to the right for each series of points, and such a correction to the 1.27- and 9.2-GHz data can be consistently chosen to remove most of the discrepancy in the scaling to the right of the minimum. The linear dependence of linewidth upon frequency, remarked upon earlier, is expressed in this plot as a frequency-independent value of the relative linewidth minimum. There is substantial scatter, $\sim\pm15\%$ in the depth of the scaled minimum, but recalling that the data are taken over a range of nearly 2 orders of magnitude in

frequency, the linear scaling of linewidth minimum with frequency is indeed well obeyed. The scatter from the scaling prediction to the left of the minimum is again reasonably explained as the consequence of the neglect of residual scattering corrections, the neglect of the effect of surface relaxation (spin and/or resistivity), which in fact have not been fully understood,[5] and possibly failure to account for the effects of exchange.[13] The scaling predicted by Eq. (34) is in fact quite well obeyed.

B. Theoretical fit

In Fig. 5 we indicate as well, by the smooth curve, a fit to the expected form Eq. (34), where a simple interpolation scheme is used for Eqs. (20) and (21) and the scattering time is supposed to be given by[15,16]

$$\frac{1}{\tau}=pT^3 . \tag{35}$$

Comparison of the results with the model requires the assumption of a value of the ratio of the spin precession frequency to the cyclotron frequency which is taken[17] as $\omega_s/\omega_c=1.6$. The fit is quite insensitive to the position of transition from the intermediate- to high-temperature regime, determined by κ/k_F; the indicated fit is for $\kappa/k_F=0.7\times10^{-3}$.

Are the parameters giving the fit of Fig. 5 reasonable? The parameter p of Eq. (35) used for the fit is $p=2.1\times10^7$ sec^{-1} K^{-3}, which may be compared with experimental and theoretical values[15,16,18] which are in the range $0.3-3\times10^7$ sec^{-1} K^{-3}. The large range reflects the large anisotropy of the scattering over the Fermi surface of aluminum, the faster rates being for electrons on the ridges of the second-zone Fermi surface and in the third zone, and the slower rates on the broad faces of the second zone. The value of p used in the fit must be considered reasonable.

The high-temperature width is dominated by the phonon relaxation [Eqs. (32) and (33)]. The fit of Fig. 5 uses a ratio $(1/T_p)/(1/\tau)=1.5\times10^{-4}$, to be compared with the estimated value [Eq. (33)] of 2×10^{-4}. The agreement is surely fortuitous since the theoretical estimate is certainly reliable to within no better than a factor of 3.

Finally, the fit implies a value for the relaxation rate in the intermediate temperature regime, [see Eq. (20b)], $(1/\omega_s T_2)=2.9\times10^{-3}$. Comparison with the model prediction requires values for the δg_0 and κ/k_F of Eq. (20). The radius κ of the R disk is taken such that $\pi\kappa^2$ is equal to the area of the Fermi surface near the R points, calculated without spin-orbit coupling, for which the crystal-field-induced gap is less than or equal to the spin-orbit gap which is 0.77×10^{-3} Ry. This estimate gives $\kappa/k_F=0.7\times10^{-3}$.

Estimates of δg_0 based simply on extrapolation of perturbation theory results for $\delta g(k)$ are of the order of 300, but use of this number underestimates the effectiveness of the R disk in dephasing the spins. The transit times through the disks are underestimated in the simple model presented above because that model does not account for the changes in group velocity resulting from the crystal-field distortions of the shape of the Fermi surface. Estimates, again treating the spin-orbit coupling as a perturbation and extrapolating into the R point, indicate a typical rms phase accumulation, Eq. (11), of 1 radian for a trajectory passing through an R point. Using these calculated phase accumulations as the basis for the identification with the formulas of the preceding section leads to the assignment $\delta g_0=1.1\times10^3$.

These parameters, $\kappa/k_F=0.7\times10^{-3}$ and $\delta g_0=1.1\times10^3$, when used in Eq. (20b) for the relaxation rate in the intermediate regime yield $1/\omega_s T_2=4.4\times10^{-3}$ in good agreement, again fortuitous, with the value 2.9×10^{-3} deduced from the fits to the data of Fig. 5. Again the estimates are not felt to be reliable to within better than a factor of 3.

The parameters $\delta g_0=1.1\times10^3$ and $\kappa/k_F=0.7\times10^{-3}$ may also be used, with the model of Sec. II, to estimate an rms variation over the Fermi surface of the g value of

$$\langle(\delta g)^2\rangle^{1/2}=\delta g_0 2\sqrt{3}\kappa/k_F=2.7$$

and of the orbitally averaged g of

$$\langle g_0^2\rangle^{1/2}=\delta g_0(4/\sqrt{\pi})(\kappa/k_F)^{3/2}=0.046 .$$

These may be compared with the values of I of 0.47 and 0.067, respectively. The first is underestimated in I because it is completely dominated by the contributions of the R disks, a fact not recognized earlier, which are poorly characterized in I. The second is in reasonable accord with the R-disk model since the orbital averaging makes the result less sensitive to neglect of the R disks. In fact, much of the rms variation of the orbitally averaged g is due to the different mean value in the second and third zones, an important bit of physics not included in the present model. In summary then, the parameters deduced from the fits to the scaled data of Fig. 5 are in quite reasonable arguement with the simple model described in Sec. II and with the magnitudes estimated here.

IV. DISCUSSION

Section III presents the main burden of the argument that the models of Sec. II give basically a satis-

factory account of the full variation with temperature and with frequency of the ESR linewidth in aluminum. This section gives a brief qualitative discussion of a few additional points.

A. Systematic deviations

Evident in Fig. 5 is a systematic decrease, with increasing frequency, of the minimum value of $1/\omega_s T_2$, the decrease being about 30% for an eightfold increase in frequency. No account has been taken in this development of magnetic breakdown across the spin-orbit gaps.[19] Breakdown should be occurring at the high fields and, because it transfers electrons between orbits of opposite sign of g shifts, tends to suppress the phase error accumulated upon transit near an R point. The breakdown is proposed as a possible source of the systematic variation noted.

As noted by a number of authors,[1,5,6] for aluminum the minimum ESR linewidth observed at any frequency is proportional to the frequency. In the model presented above this result is an immediate consequence of the scaling illustrated in Fig. 5. Plots of minimum width versus frequency will be influenced to some degree, however, by the fact that for the lowest-frequency data[1] the residual scattering has prevented attainment of the $\omega_c\tau$ required to reach the minimum, and for the high-frequency points there may be some systematic variation, as noted in the preceding paragraph, due to magnetic breakdown.

Lubzens[1] and co-workers and Dunifer and Pattison[5] have also noted that in the regime in which $1/T_p$ dominates the linewidth, the widths at a fixed temperature fit well to a linear dependence on frequency plus a constant, with the slope of the linear frequency dependence being higher at the higher temperature. Rather than attributing this effect to a frequency dependence of the phonon relaxation, we would note that the motional narrowing model presented above in fact accounts qualitatively for this observation. At the temperatures 50 and 80 K for which Dunifer and Pattison[5] have plotted the frequency dependence of the linewidth, $\omega_c\tau$ for 79-GHz data is still in the intermediate regime of Eqs. (20), while the 1.27-GHz data are in the high-temperature regime, particularly at 80 K, and thus in the classical motionally narrowed regime. This gives an additional temperature dependence which is more marked at 80 K than at 60 K and which accounts satisfactorily for the observations.

B. T_1 and T_2 at low temperatures

The discussion above has focused rather arbitrarily on motional narrowing arguments for the linewidth $1/T_m$, with additional comments concerning one T_1 mechanism, the spin flips associated with the scattering between states with different degrees of spin-orbit mixing of spin-up and spin-down states.[14] There is an additional T_1 mechanism, clearly related to the $1/T_m$ result discussed above. As noted briefly earlier, the g-shift tensor near the R points has off-diagonal elements as well as diagonal elements. The diagonal elements, as modulated by the combination of cyclotron motion and scattering, give a spectral density of fluctuating fields parallel to the applied field which were discussed in conjunction with Fig. 4. This spectral density at $\omega=0$ determines the motionally narrowed linewidth. The off-diagonal elements have a similar spectrum, and will induce spin flips at a rate proportional to the spectral density at the Larmor frequency ω_s which contribute both to $1/T_2$ and to $1/T_1$. In the intermediate and high-temperature regimes, with the spectral peaks of Fig. 4 heavily overlapping, the spectral density at $\omega=\omega_s$ will be the same as at $\omega=0$, and the contributions to $1/T_1$ and $1/T_2$ will be equal, as is conventionally assumed for the electron spins in metals. In the low-temperature regime, however, this will no longer be the case since ω_c is substantially different from ω_s, and one may expect $1/T_1 \ll 1/T_2$ as $(\omega_c\tau)^{-1}$ becomes small compared with $|\omega_s-\omega_c|/\omega_c$, leaving the spectral density peak centered at ω_c well isolated from the Larmor frequency ω_s.

C. Improved calculations

The discussion presented here is based on a very simple model with numerical estimates based on perturbation-theory results. The basic physical ideas are felt to be sound and to offer the essentials of the understanding of the temperature and frequency dependence of the aluminum linewidth in the regime in which electron-electron exchange is not playing an important role. The quantitative estimates are of course crude, and it is unlikely that they are reliable to within better than a factor of 3.

Improvement in the calculations requires the full solution of the g-shift problem near the R points, treating the spin-orbit gap properly, and taking full account of the distortions from sphericity of the Fermi surface. Because the bulk of the contributions to the relaxation comes specifically from the immediate neighborhood of the R points much insight could be gained by focusing attention entirely here, without need for tedious integrations over the full Fermi surface. At the same time, the problem of magnetic breakdown would also have to be seriously addressed.

V. CONCLUSIONS

Calculations of the g anisotropy in aluminum[6] have been exploited and extended to develop a semiquantitative understanding of the full frequency and temperature dependence of the ESR linewidth in aluminum, including both the motional narrowing regime and the phonon-dominated regime. The following points should be noted:

(1) The model predicts a scaling which is well, though not perfectly, obeyed.

(2) The parameter values giving a reasonable fit to the scaled data agree with estimates based on the model to better than the estimated precision of a factor of 3 in the model values.

(3) The linear dependence on frequency of the minimum linewidth is a natural outcome of the model.

(4) Systematic deviations from the scaling may be qualitatively understood in terms of residual scattering contributions to $1/\tau$ and the effects of magnetic breakdown.

(5) An apparent frequency dependence of the phonon spin-flip scattering can be understood as a consequence of the motional narrowing model, with the phonon-induced relaxation remaining independent of frequency.

(6) The model predicts that at low temperatures, for $\omega_c\tau \gg 1$, T_1 should become long compared with T_2 for conduction electrons in high-purity aluminum.

(7) Further refinement of these ideas requires exact treatment of the spin-orbit interaction near the R points of the Fermi surface and detailed consideration of the effects of magnetic breakdown.

ACKNOWLEDGMENTS

This work has been supported in part (R.H.S.) by the National Science Foundation through Contract No. DMR-80-08546, and through the Cornell University Materials Science Center Report No. 4885.

[1]D. Lubzens, M. R. Shanabarger, and S. Schultz, Phys. Rev. Lett. 29, 1387 (1972); D. Lubzens and S. Schultz, *ibid.* 36, 1104 (1976).

[2]J. P. Long and R. H. Silsbee, Phys. Rev. B (in press).

[3]J. R. Sambles, G. Sharp-Dent, J. E. Cousins, A. Stesmans, and J. Witters, Phys. Status Solidi B 79, 645 (1977).

[4]J. van Meijel, A. Stesmans, and J. Witters, Solid State Commun. 21, 753 (1977).

[5]G. L. Dunifer and M. R. Pattison, Phys. Rev. B 14, 945 (1976).

[6]F. Beuneu, J. Phys. F 10, 2875 (1980); F. Beuneu, Ph.D. thesis, Université de Paris-Sud, 1979 Report No. CEA-R-5026 (unpublished). Many additional references to experimental results on aluminum are given in this thesis.

[7]R. Dupree and B. W. Holland, Phys. Status Solidi 24, 275 (1967).

[8]N. W. Ashcroft, Philos. Mag. 8, 2055 (1963).

[9]Y. Yafet, Solid State Phys. 14, 1 (1963).

[10]F. Beuneu and P. Monod, Phys. Rev. B 18, 2422 (1978); P. Monod and F. Beuneu, *ibid.* 19, 911 (1979).

[11]A. Abragam, *The Principles of Nuclear Magnetism,* (Oxford University Press, Oxford, 1961), pp. 432 and 433.

[12]C. P. Slichter, *Principles of Magnetic Resonance* (Harper and Row, New York, 1963).

[13]R. Freedman and D. R. Fredkin, Phys. Rev. B 11, 4847 (1975); D. R. Fredkin and R. Freedman, Phys. Rev. Lett. 29, 1390 (1972).

[14]R. J. Elliott, Phys. Rev. 96, 266 (1954).

[15]A. B. Meador and W. E. Lawrence, Phys. Rev. B 15, 1850 (1977).

[16]D. K. Wagner and R. Bowers, Adv. Phys. 27, 651 (1978).

[17]F. W. Spong and A. F. Kip, Phys. Rev. 137, A431 (1965).

[18]T. Wegehaupt and R. E. Doezema, Phys. Rev. B 18, 742 (1978); W. Mohr and J. S. Lass, *ibid.* 19, 6244 (1979).

[19]A. B. Pippard, Proc. R. Soc. London, Ser. A 270, 1 (1962); 287, 165 (1965).